Evaluation of the coupling parameters of many-body interactions in Fe(110)

X. Y. Cui,[1,*] K. Shimada,[2,†] Y. Sakisaka,[3] H. Kato,[3] M. Hoesch,[4] T. Oguchi,[5,‡] Y. Aiura,[6] H. Namatame,[2] and M. Taniguchi[1,2]

[1]*Graduate School of Science, Hiroshima University, Kagamiyama 1-3-1, Higashi-Hiroshima 739-8526, Japan*

[2]*Hiroshima Synchrotron Radiation Center, Hiroshima University, Kagamiyama 2-313, Higashi-Hiroshima 739-0046, Japan*

[3]*Faculty of Science and Technology, Hirosaki University, Hirosaki, Aomori 036-8560, Japan*

[4]*Diamond Light Source, Didcot OX11 0DE, United Kingdom*

[5]*ADSM, Hiroshima University, Kagamiyama 1-3-1, Higashi-Hiroshima 739-8530, Japan*

[6]*National Institute of Advanced Industrial Science and Technology, Tsukuba, Ibaraki 305-8568, Japan*

(Received 22 August 2010; published 29 November 2010)

In order to clarify many-body interactions in ferromagnetic iron, we performed high-resolution angle-resolved photoemission spectroscopy (ARPES) on a Fe(110) single crystal. We quantitatively analyzed the ARPES line shapes for a majority-spin band crossing the Fermi level (E_F). The observed group velocity was reduced with respect to the band-structure calculation by a factor of 1/2.7, giving a coupling parameter due to the electron-electron interaction of $\lambda_{ee}=1.7\pm0.1$. This suggests a strong electron correlation in Fe 3*d*, which is consistent with recent high-resolution ARPES results. The real and imaginary parts of the self-energy have been experimentally evaluated near E_F. The coupling parameter of the electron-phonon interaction was estimated to be $\lambda_{ep}=0.16\pm0.02$, which is 1/10 of λ_{ee}. The effective-mass enhancement with respect to the band mass $m^*/m_b\sim1+\lambda_{ee}+\lambda_{ep}\sim3$ was, therefore, mainly caused by electron correlation.

DOI: 10.1103/PhysRevB.82.195132 PACS number(s): 75.50.Bb, 79.60.−i, 71.18.+y, 75.10.Lp

I. INTRODUCTION

Many-body interactions involving electrons in solids are directly related to a large variety of physical properties.[1] The magnitudes of these interactions can be measured by a dimensionless coupling parameter $\lambda=-(\partial\,\mathrm{Re}\,\Sigma/\partial\omega)_{\omega=0}$, where $\mathrm{Re}\,\Sigma$ is the real part of the self-energy. Due to these many-body interactions, the Fermi velocity (v_F) is reduced by the renormalization factor $Z=1/(1+\lambda)$. The electron effective mass (m^*), on the other hand, increases with respect to the band mass without many-body interactions (m_b) by a factor of $m^*/m_b=1/Z$. The lifetime of interacting electrons (quasiparticles) near the Fermi level (E_F) is given by $\tau=\hbar/2|\mathrm{Im}\,\Sigma|$, where $\mathrm{Im}\,\Sigma$ is the imaginary part of the self-energy. Since $\mathrm{Re}\,\Sigma$ and $\mathrm{Im}\,\Sigma$ are related via the Kramers-Kronig transform, the magnitude of λ also gives a measure of the quasiparticle's lifetime.

High-resolution angle-resolved photoemission spectroscopy (ARPES) is among the most powerful tools available to directly clarify the detailed electronic structure of solids.[2] The reduction in v_F by coupling to the many-body interactions can be observed as a *kink structure* in the energy-band dispersion.[3] Using detailed analysis of the ARPES spectral line shapes, one can, in principle, experimentally evaluate λ at a given point on the Fermi surface (FS).[2–12] This is one of the most significant advantages of high-resolution ARPES over other experimental methods in Fermiology.

In the present paper, we will examine many-body interactions in a ferromagnetic iron single crystal using high-resolution ARPES. The electronic band structure of Fe has been studied extensively, both theoretically[13,14] and experimentally.[15–28] Earlier ARPES results seemed to agree with those of band-structure calculations using the local-spin-density approximation (LSDA).[15,16,22] The deviation between experiment and theory was reported to be ~10% at high-symmetry points.[17,22] The band points at these high-symmetry points were determined from the peak positions in the energy distribution curves (EDCs).

Recently, Schäfer *et al.* extensively studied Fermi surfaces and energy-band dispersions using Fe(110) thin films grown on a W(110) substrate.[23,24] The observed Fermi surfaces coincided well with the theoretical ones. However, the group velocity near E_F was significantly reduced, and the effective-mass enhancement factors were evaluated to be $1+\lambda=1.1-3.6$. The effective mass enhancement factor depended upon the Fermi surface sheet, spin, and *k* direction.[24] The largest value was close to that of Ni, $1+\lambda=1.9-2.8$,[7] implying that the many-body interactions in Fe are significant. However, no clear satellite structure has been identified in the core levels of clean Fe (Refs. 20 and 29) while a 6 eV satellite exists in the core-level and valence-band spectra of Ni (Ref. 30). Except for the significant reduction in the Fermi velocity with respect to the calculated one, the observed band points at the high-symmetry points were not significantly different, which is in agreement with previous ARPES results.[24]

Since the magnetic moment of Fe ($\mu=2.1\ \mu_B$) (Ref. 13) is the largest among the 3*d* transition-metal elements, one may expect to observe traces of the electron-magnon interaction in high-resolution ARPES measurements. Schäfer *et al.*[23] found a kink structure and a reduction in the experimentally determined $2|\mathrm{Im}\,\Sigma|$ below the binding energy of ~160 meV for the surface-derived states of Fe. It was argued that the kink structure originated from an electron-magnon interaction. The spin-polarized electron energy-loss spectra indicated a peak structure in the energy range of 100–350 meV due to spin-wave excitation.[31–33] If electrons are scattered by magnons (spin waves), it is reasonable to assume that a kink structure caused by this electron-magnon interaction should exist in the above energy range.

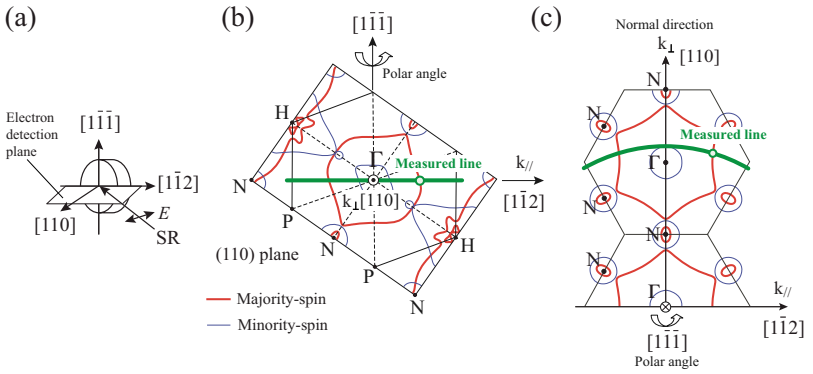

FIG. 1. (Color online) (a) Geometry of the present ARPES measurements. Calculated FSs in (b) the (110) plane and (c) the ($\bar{1}$11) plane. ARPES measurements were performed along the line shown in (b) and (c).

Theoretical calculations of the magnon density of states (DOS) in bulk Fe, on the other hand, indicated a well-defined cutoff around 340 meV.[34] Furthermore, neutron-scattering experiments and theoretical calculations indicated that the boundary between the optical and acoustic magnon branches was unclear.[35–38] Naito and Hirashima[39] calculated the self-energy derived from the electron-magnon interaction in Fe, and indicated that the renormalization caused by the electron-magnon interaction is insufficient to form a kink structure. The details of the electron-magnon interaction in the bulk-derived Fe bands remains to be addressed. Recent spin-polarized electron energy-loss spectroscopy indicated that the energy scales of magnon dispersion at the surface and in the bulk are different.[33]

In order to quantitatively study many-body interactions in iron, we performed high-resolution low-temperature ARPES measurements on a Fe(110) bulk single crystal, using tunable photon energies.[26–28] In our previous line-shape analysis using momentum distribution curves (MDCs), we found a broad kink structure at ~−270 meV, and interpreted it as evidence of the electron-magnon coupling.[28] However, though the line-shape analysis based on the MDC is effective near E_F, we have recently realized its limitations at energies far from E_F if the spectral linewidth is significantly broadened with decreasing energy.

In this study, we re-examined the ARPES line shapes, clarifying the validity of the MDC and EDC analyses. The magnitudes of the coupling parameters for the electron-phonon (λ_{ep}) and electron-electron (λ_{ee}) interactions were evaluated quantitatively. We confirmed a significant effective mass enhancement with respect to the band mass given by the band-structure calculation near E_F, in agreement with Fe film results.[24,25] We could not, however, confirm the kink structure derived from the electron-magnon interaction in the limited energy range we could examine. Present study suggests that despite the inevitable $\delta k_\perp$ broadening in the photoemission process from three-dimensional electron systems, we can, by selecting a suitable point in the momentum space, evaluate the self-energy derived from the many-body interactions in detail.

II. EXPERIMENT

An Fe(110) single crystal was cleaned by repeated cycles of Ar^+ ion sputtering and subsequent annealing at 570 °C for 30 min.[26–28] The cleanliness of the sample surface was verified by Auger electron spectroscopy and ultraviolet photoemission spectra. The carbon contamination consisted of less than 1%, nitrogen, and the oxygen and sulfur concentrations were below the detection limit.

The ARPES measurements were carried out at the linear undulator beamline BL-1 at the Hiroshima Synchrotron Radiation Center (HSRC), Hiroshima University.[40] A multichannel angular mode of the hemispherical electron energy analyzer (ESCA200, VG-SCIENTA) was used for high-resolution ARPES measurements. The total-energy resolution was set to ΔE=15 meV ($h\nu$=40.5 eV) and the angular resolution was $\Delta\theta$=0.3° (Δk=0.016 Å^{-1}). The sample was mounted on a low-temperature goniometer (R-Dec Co. Ltd., i-GONIO LT) (Ref. 41) and cooled to ~90 K.[42] The base pressure of the main chamber was below 1×10^{-10} Torr.

The parallel and perpendicular components of the photoelectron wave vectors relative to the sample surface, $k_\parallel$ and $k_\perp$, were determined from the equations $k_\parallel=\sqrt{\frac{2mE_k}{\hbar^2}}\sin\theta$ and $k_\perp=\sqrt{\frac{2m}{\hbar^2}(E_k\cos^2\theta+V_0)}$, where E_k is the kinetic energy of the photoelectron and V_0 is the inner potential.[43] Here, we assumed V_0=8.9 eV, which was determined for bulk Fe(110).[19,44] The detection plane of the electron energy analyzer, the electric vector of the incident synchrotron radiation, and the [1$\bar{1}$2]($=k_\parallel$) direction of the sample were all in the same plane [Fig. 1(a)]. The polar angle of the sample was defined by the rotation around the [1$\bar{1}\bar{1}$] direction in $k_\parallel$ scans covering the line shown in Figs. 1(b) and 1(c). Figures 1(b) and 1(c) show calculated FSs originating from the majority-spin (thick contours in red) and minority-spin (thin contours in blue) states[45] that can be examined using Fe(110) in the present geometry.

We observed several energy bands crossing E_F in Fe(110), by changing the detection angles and incident photon energies. Most of these bands had a broad spectral width, which was assumed to derive from the final-state or matrix-element effects.[46–49] For quantitative line-shape analysis, an energy band with a narrow linewidth over a structure-free background is favorable. Such a narrow peak was found at the photon energy of $h\nu$=40.5 eV, where the observed MDCs close to E_F were highly symmetric, further indicating that a position in momentum space is suitable for a quantitative analysis. We therefore selected an incident photon energy of $h\nu$=40.5 eV, and examined the energy band along the measured lines in Figs. 1(b) and 1(c). Figure 2 shows calculated

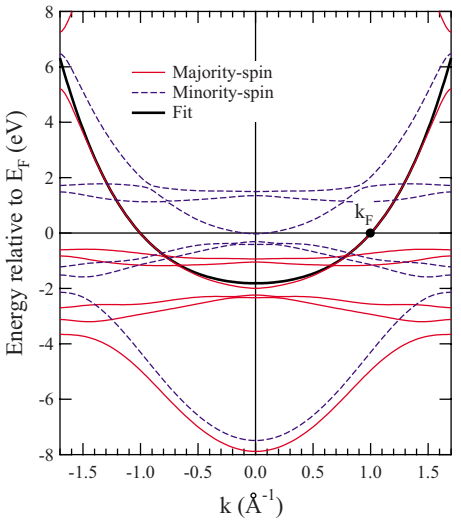

FIG. 2. (Color online) Calculated energy-band dispersion along the line shown in Fig. 1. The thick solid line indicates a fit to $f(k)=a_0+a_1k^2+a_2k^4$ near E_F.

band dispersions along the measured line in Figs. 1(b) and 1(c). A majority-spin band crosses E_F at the Fermi wave number of $k_F \sim 1.0$ Å^{-1}.

We should note that the measured line was close to the ΓHPN plane, which is the mirror plane of the Fermi surface. As $(\partial\varepsilon_k/\partial k_\perp)\sim 0$ near the mirror plane, the final state broadening due to the dispersion relation[47,48] was expected to be $\delta E=(\partial\varepsilon_k/\partial k_\perp)\cdot\delta k_\perp \sim 0$. Furthermore, as the $k_\perp$ direction was nearly parallel to the Fermi surface plane, $\delta k_\perp$ should not give a large $\delta k_\parallel$ (=MDC width) near E_F. These are the possible reasons that we were able to observe a narrow spectral linewidth at $h\nu \sim 40.5$ eV. One-step photoemission calculations may be required to arrive at a quantitative explanation of this observation.[50,51]

Figures 3(a) and 3(b) show the EDCs and an intensity plot of the ARPES results, respectively. Here, the wave number was measured with respect to k_F for the detailed analysis.

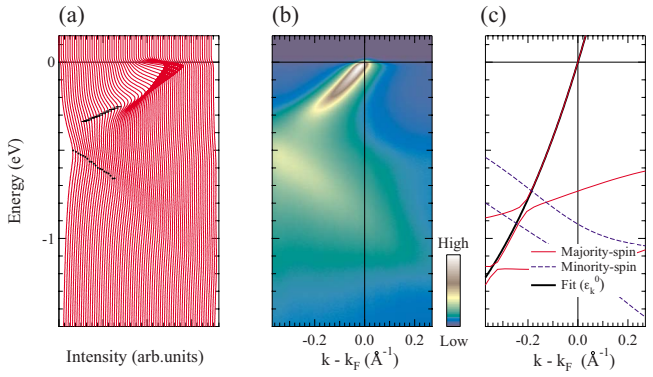

FIG. 3. (Color online) (a) EDCs taken at $h\nu=40.5$ eV with wave numbers from $k-k_F=-0.37$ Å^{-1} (left) to 0.27 Å^{-1} (right). Bars and filled circles indicate peak positions in EDCs. (b) Intensity plot corresponding to (a). (c) Calculated energy-band dispersions to be compared with (a) and (b). We fit the theoretical energy-band crossing E_F to a function $\varepsilon_k^0=a_0+a_1(k-k_F)^2+a_2(k-k_F)^4$, and assumed a noninteracting band in the line-shape analysis.

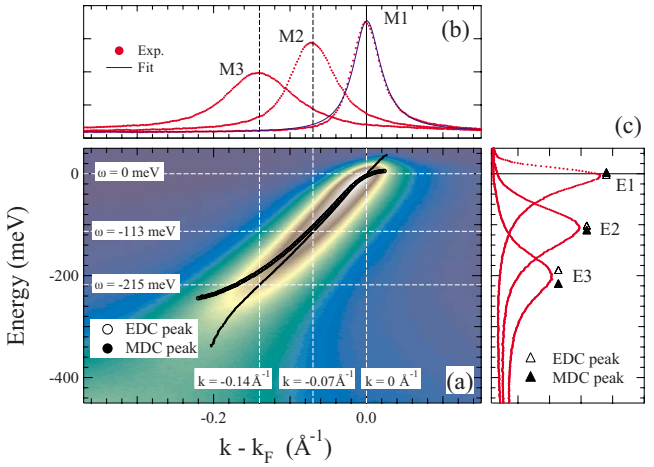

FIG. 4. (Color online) (a) ARPES intensity plot of Fe(110) taken at $h\nu=40.5$ eV near E_F. We divided the ARPES intensity by the Fermi-distribution function to correct for the steplike cutoff at E_F. Open and filled circles indicate peaks evaluated by EDC and MDC analyses, respectively. (b) MDCs at $\omega=0$ (M1), −113 (M2), and −215 (M3) meV. (c) EDC at $k-k_F=0$ (E1), −0.07 (E2), and −0.14 (E3) Å^{-1}, where the MDCs reach a maximum. Filled and open triangles indicate peak positions in the EDCs and those estimated by the MDC peaks, respectively.

Bars (filled circles) in Fig. 3(a) indicate peak positions of EDCs which should be compared with the calculated majority (minority)-spin band points in Fig. 3(c). It can be clearly seen that the Fermi velocity was markedly reduced, and the spectral intensity decreased rapidly with decreasing energy. In the following sections, we will quantitatively analyze ARPES line shapes and evaluate the self-energy.

In our recent work on Ni(110),[50] we have observed *ghost structures* that did not correspond to the initial states expected from the transition into the free-electronlike final states. These structures were derived from the final-state wave function that was composed of several Bloch waves with different $k_\perp$ whose contribution strongly depended on the details of the matrix elements. The origin of the structure can be explained based on the one-step photoemission calculation.[50] We did not observe, however, this kind of structure in our previous studies on Ni(110) examining different points in the momentum space,[7,49] as well as in Figs. 3(a) and 3(b) in this study. Note also that one-dimensional DOS derived from the $k_\perp$ broadening[52] was not significant judging from the weak Fermi edge intensity away from k_F.

III. RESULTS

Figures 4(a)–4(c) show the intensity plots, the MDCs (M1, M2, M3) at $\omega=0(E_F)$, −113, −215 meV and EDCs (E1, E2, E3) at the MDC peak positions. In order to eliminate the steplike spectral feature due to the Fermi edge, we divided the spectra by the Fermi-Dirac distribution function.

In Fig. 4(b), the MDCs are very close to symmetric Lorentzian functions. This indicates that the $k_\perp$ dispersion effect on the line shape was negligible,[49] and that the self-energy was almost k independent (Appendix A). We should

also note that the background is structureless and the intensity is much smaller than the MDC peak intensity. In order to precisely determine the peak positions, we used the asymmetric function $L(\omega)=\frac{\Gamma(1-\alpha)\cos[\pi\alpha/2+(1-\alpha)\arctan(\omega/\gamma)]}{(\omega^2+\gamma^2)^{(1-\alpha)/2}}$ (Ref. 53). The asymmetric distortion was measured by α, and in the case of $\alpha=0$, the line shape was reduced to a Lorentzian, $L(\omega)=\frac{\gamma}{\omega^2+\gamma^2}$, where γ is the linewidth. In this analysis, $|\alpha|$ was evaluated to be 0.01–0.06. Figure 4(b) shows the resulting band positions.

The MDC width at E_F was determined to be 0.046 Å^{-1}. If the final state broadening was negligible, it is reasonable to assume that the MDC width was mainly determined by the electron-impurity scattering. Based on the uncertainty principle, $\delta x\cdot\delta p=\delta x\cdot\hbar\,\delta k\sim\hbar$, the mean-free path of the electron is found as $\delta x=1/\delta k\sim 22$ Å. The group velocity at E_F according to the MDC analysis was $v_F=(1/\hbar)(\partial\varepsilon_k/\partial k)_{\omega=0}=2.5\times10^5$ m/s. The upper limit of lifetime (or relaxation time) of a quasiparticle was therefore estimated as $\tau=\delta x/v_F=1/(\delta k\cdot v_F)=1\times10^{-14}$ s.

The EDC linewidth became narrower as the peak approached E_F. We evaluated the EDC peaks using the same asymmetric function, as in the MDC analysis [Fig. 4(b)]. The line shape at ~−50 meV was too complex to be fit properly (mainly due to the electron-phonon interaction, and the peak position error was 5–10 meV. Deviations in the energy-band dispersions given by the EDC and MDC analyses were evident, especially near E_F and below ~−120 meV.

The strong kink near E_F in the dispersion evaluated from the EDCs mainly originated from the truncation of the spectral intensity above E_F because of the Fermi cutoff. One cannot, therefore, rely on the band dispersion determined by EDC analyses near E_F. MDC analysis provides more accurate band positions.

On the other hand, at lower energies, below ~−200 meV, the dispersion evaluated from the MDCs formed a broad kink structure while the dispersion evaluated from the EDCs was parabolic. As clearly shown in Fig. 4(c), MDC analysis cannot provide the correct peak positions in the EDC spectra, especially at lower energies [see E3 in Fig. 4(c)]. This is because of a geometric effect related to the significant energy-dependent linewidth broadening (Appendix B), and suggests that MDC analysis is invalid below a certain energy. After shifting the EDC peaks by +0.005 Å^{-1}, they coincided well with the MDC peaks for energies ranging from −50 to ~−120 meV (Fig. 5). We therefore assumed that the MDC analysis was only valid from E_F down to ~−120 meV.

Based on the band dispersion determined by EDC analysis at least, there was no evidence for the kink structure corresponding to the electron-magnon interaction in the energy range from E_F down to ~−300 meV [Fig. 3(a)]. The broad kink in the band dispersion at ~−270 meV determined by the MDC analysis was most probably related to the significant energy-dependent linewidth broadening, not to the electron-magnon interaction.

IV. DISCUSSION

A. Self-energy and coupling parameter

The ARPES spectrum corresponds to the quasiparticle spectral function,[2]

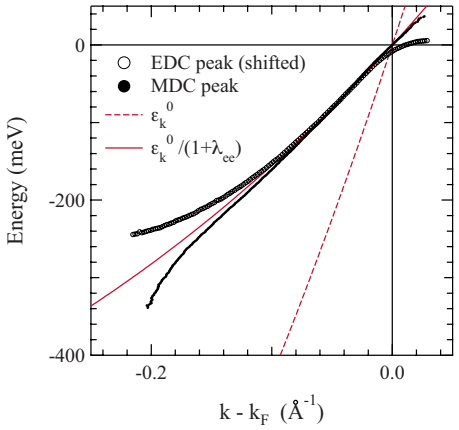

FIG. 5. (Color online) Experimental band positions near E_F obtained by EDC and MDC analysis. The EDC points were shifted by +0.005 Å^{-1}. The dashed line represents the energy-band dispersion (ε_k^0) given by the band-structure calculation. Multiplying by a factor of $1/(1+\lambda_{ee})$, the theoretical dispersion (solid line) reproduces the experimental values from E_F down to ~−120 meV.

$$A(k,\omega)=-\frac{1}{\pi}\frac{\mathrm{Im}\,\Sigma(k,\omega)}{[\omega-\varepsilon_k^0-\mathrm{Re}\,\Sigma(k,\omega)]^2+[\mathrm{Im}\,\Sigma(k,\omega)]^2}. \quad (1)$$

Since we observed nearly symmetric MDCs in this study, we assumed that the k dependence of the self-energy was negligible so that $\Sigma(k,\omega)\sim\Sigma(\omega)$ (Appendix A). One can evaluate $2|\mathrm{Im}\,\Sigma|$ and $\mathrm{Re}\,\Sigma$ experimentally using the spectral width ($\Gamma=\delta E=2|\mathrm{Im}\,\Sigma|$) and the energy shift from the noninteracting band, ε_k^0. $\mathrm{Re}\,\Sigma$ can be obtained from the expression $\mathrm{Re}\,\Sigma(\varepsilon_k^*)=\varepsilon_k^*-\varepsilon_k^0$, where ε_k^* is the observed energy of the band points.[3]

First, we examined the electron-electron interaction based on the difference between the experimental group velocity and the theoretical one determined using the LDA calculation.[45] We fit the calculated band dispersion along the measured line from −0.6 to +0.4 eV with a function, $\varepsilon_k^0=a_0+a_1(k-k_F)^2+a_2(k-k_F)^4$, and regarded it as a noninteracting band. We found that values of $a_0=-1.8143$ eV, $a_1=1.2618$ eV Å^2, and $a_2=0.53715$ eV Å^4 could reproduce the theoretical energy-band dispersion reasonably well, not only near E_F but over a wide energy range (see thick black line in Fig. 2).

The group velocity given by the band-structure calculation, $v_F^0=7.1\times10^5$ m/s, was larger than the observed value of $v_F\sim2.5\times10^5$ m/s. We assumed that the observed band dispersion was narrowed by $1/(1+\lambda_{ee})$ compared with that given by the LSDA calculation because of renormalization due to the electron-electron interaction. We reproduced the experimental energy-band dispersion by $\varepsilon_k^0/(1+\lambda_{ee})$ with $\lambda_{ee}=1.7\pm0.1$ (solid line in Fig. 5), for the energy range from E_F down to −120 meV.

Since the Debye temperature of Fe is 470 K (Debye energy: $k_B\Theta_D=40$ meV),[54] there may exist a kink structure due to the electron-phonon interaction in the energy range of $0\le|\omega|\le40$ meV.

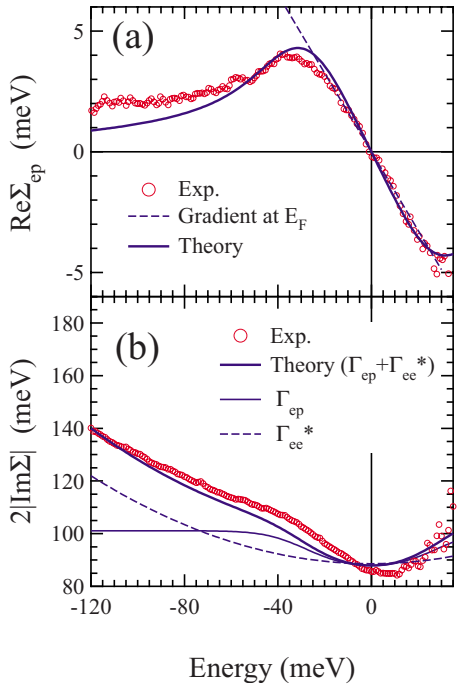

FIG. 6. (Color online) (a) Experimental Re Σ_{ep} (open circles) compared with the calculated one (solid line). The dashed line indicates the gradient of the experimental Re Σ_{ep} at E_F. (b) Experimental $2|\mathrm{Im}\,\Sigma|$ (open circles) compared with the theoretical Γ_{ep} (solid line). The dashed line indicates a fit to $2\beta^*\omega^2$, which gives the linewidth broadening Γ_{ee}^*.

In order to evaluate the real part of the self-energy due to the electron-phonon interaction (Re Σ_{ep}), we subtracted the renormalized theoretical band dispersion $\varepsilon_k^* = \varepsilon_k^0/(1+\lambda_{ee})$ from the experimental one. As for the spectral linewidth, we used the formula $\Gamma(\omega) = (\partial\varepsilon_k/\partial k)\cdot\delta k$,[55] where δk represents the MDC width. For the evaluation of $2|\mathrm{Im}\,\Sigma_{ep}|$, we assumed that the electron-phonon interaction was independent of the electron-electron interaction.

Figures 6(a) and 6(b) show the resulting real and imaginary parts of the self-energy. There is a clear peak at ~ -40 meV in Re Σ_{ep}, and a rapid decrease in the linewidth above -40 meV in $2|\mathrm{Im}\,\Sigma_{ep}(\omega)|$. We should note that the experimental $2|\mathrm{Im}\,\Sigma(\omega)|$ is on a constant background ~ 85 meV. It was mostly determined by δk at E_F and the magnitude of the Fermi velocity, $\Gamma_0 = \delta k\cdot\hbar v_F = 0.046$ Å^{-1} $\times 1.7$ eV Å ~ 80 meV. Figure 6(a) shows experimentally obtained Re Σ_{ep}. The contribution from Re Σ_{ee} was already subtracted as we evaluated the energy shifts from the renormalized energy-band dispersion, ε_k^*. In order to confirm the self-energy resulting from the electron-phonon interaction, we calculated the lifetime broadening using the formula,[3,56]

$$\Gamma_{ep}(\omega,T) = 2|\mathrm{Im}\,\Sigma_{ep}(\omega,T)| = 2\pi\int_0^\infty \alpha^2F(\nu)[2n(\nu,T) + f(\nu+\omega,T) + f(\nu-\omega,T)]d\nu, \quad (2)$$

where $n(\nu,T)$ and $f(\nu,T)$ are the Bose-Einstein and Fermi-Dirac distribution functions, respectively. Since the Eliashberg function, $\alpha^2F(\nu)$, for Fe has not yet been theoretically provided, we used the theoretical phonon DOS for $F(\nu)$ and regarded α^2 as an adjustable parameter. According to microcontact spectroscopy of Fe, α^2 as a function of energy forms a broad maximum centered at ~ 20 meV.[57] If we assume α^2=constant, we may overestimate the contributions from the acoustic phonons near $\omega\sim 0$ and the optical phonons near $\omega\sim k_B\Theta_D$. The real part of the self-energy Re Σ_{ep} can be calculated using $|\mathrm{Im}\,\Sigma_{ep}|$ because the two are mutually related via the Kramers-Kronig transform.[3]

The calculated Re Σ_{ep} and $2|\mathrm{Im}\,\Sigma_{ep}|$ are shown in Figs. 6(a) and 6(b). The peak structure at ~ -40 meV in the experimental Re Σ_{ep} was explained well by the calculated Re Σ_{ep}. Also the reduction in $2|\mathrm{Im}\,\Sigma_{ep}|$ above ~ -40 meV was reproduced by the theoretical calculation. These observations confirm that the kink structure at ~ -40 meV does originate from the electron-phonon interaction.

Based on the gradient of the experimental Re Σ_{ep} near E_F [dashed line in Fig. 6(a)], the coupling parameter of the electron-phonon interaction was estimated as $\lambda_{ep} = 0.16 \pm 0.02$. Although we estimated the coupling parameter at ~ 90 K, it should be almost the same as the value at 0 K (Appendix C). Therefore, the coupling parameter for the electron-phonon interaction was only $\sim 1/10$ of that for the electron-electron interaction.

The observed $2|\mathrm{Im}\,\Sigma|$ further increased below $\omega\sim -40$ meV because of lifetime broadening due to the electron-electron interaction following $\Gamma_{ee}^*(\omega) = 2|\mathrm{Im}\,\Sigma_{ee}(\omega)|/(1+\lambda_{ee})$ (Appendix A). The energy dependence of $2|\mathrm{Im}\,\Sigma_{ee}|$ is given by $2\beta[(\pi k_BT)^2+\omega^2]$,[1,3] which exhibits ω^2 dependence at low temperatures in accordance with the Fermi-liquid theory. The dashed line in Fig. 6(b) represents a fit of Γ_{ee}^* to $2\beta^*\omega^2$ for $\omega < -40$ meV, and we obtained $2\beta^* = 2.7 \pm 0.2$ eV^{-1}. Therefore, the energy dependence of the self-energy derived from the electron-electron interaction can be given by $\mathrm{Im}\,\Sigma_{ee}(\omega) = -\beta^*(1+\lambda_{ee})[(\pi k_BT)^2+\omega^2] = -\beta[(\pi k_BT)^2+\omega^2]$, where $\beta = \beta^*(1+\lambda_{ee}) = 3.6 \pm 0.2$ eV^{-1}.

B. Effective-mass enhancement factor

In this study, the mass enhancement factor due to the electron-electron interaction was evaluated as $1+\lambda_{ee} = 2.7$, which is in the range of the previously obtained values, 2.0–3.6, for the same majority-spin FS with a different k direction.[24] The effective-mass enhancement due to the electron-electron and electron-phonon interactions at E_F was evaluated as $m^*/m_b = 1+\lambda_{ee}+\lambda_{ep} = 2.9$ for the energy band we examined. This value was nearly equivalent to those in Ni ($m^*/m_b = 1.9$–2.8),[7] suggesting that electron correlation in the Fe valence band is significant. The effective-mass enhancement of Fe estimated in the present study was close to the largest estimate determined by de Haas–van Alphen (dHvA) measurements, $m_{\mathrm{dHvA}}/m_b = 1$–$3$.[58]

Elaborate theoretical efforts, taking into account electron correlation, have provided the renormalization factors $Z^{th} = 1/(1+\lambda_{ee}^{th}) = 0.52$–$0.58$ (Ref. 59), 0.66 (Refs. 60 and 61), and 0.7 (Ref. 62). The effective-mass enhancement factor

becomes $1+\lambda_{ee}^{th}=1.4-1.9$, giving the coupling parameter $\lambda_{ee}^{th}=0.4-0.9$. These results are consistent with the reduction in the observed band energy at high-symmetry points.[24] However, the experimental coupling parameter determined from the Fermi velocity ($\lambda\sim 2$) was approximately two to four times larger than these theoretical values.

Sánchez-Barriga *et al.*[25] performed detailed spin- and angle-resolved photoemission spectroscopies on a Fe(110) thin film, and compared the results with state-of-the-art theoretical calculations taking into account many-body interactions and using a one-step model for the photoemission process. The experimental mass renormalization was much larger than the sophisticated theoretical approach but the reason for this deviation is not yet clear.

On the other hand, Walter *et al.*[63] theoretically considered mass renormalization and claimed that a theoretical Fermi velocity being compared with ARPES measurements should be reduced, taking into account spin-orbit splitting, final-state transitions, and final-state broadening. The mass renormalization values given by Schäfer *et al.* were therefore overestimated by 60% on average.[63] However, their model calculation did depend partly on empirical parameters obtained from ARPES results.

Although the reasons why the effective mass was so strongly enhanced have not been clearly elucidated, it may be helpful to summarize the observed energy shift or Re Σ_{ee} over a wide energy range, as clarified by ARPES. Near E_F, we have Re $\Sigma_{ee}\sim-\lambda\omega$ ($\omega<0$) and $\lambda\sim 2$. At high-symmetry points, such as the Γ point, Re $\Sigma_{ee}\sim 0$ or even <0. In this study, for example, we examined an energy band corresponding to the $\Gamma'_{25\uparrow}$ at the Γ point. The observed band energy for $\Gamma'_{25\uparrow}$ was determined to be −2.35 (Ref. 17), −2.6 (Ref. 18), and −2.7 eV (Ref. 21), which should be compared to the calculated values −2.25 (Ref. 13) and −2.2 eV (Ref. 24). The observed band energy was lowered by 4–23 % at the Γ point, which is opposite to the energy elevation by 64% near E_F.

If Re $\Sigma_{ee}<0$ is realized at high-symmetry points, Re Σ_{ee} should cross zero in the energy range $\mu<\omega<0$, where μ is the band energy at the high-symmetry point. Here we assume that $\omega=\zeta$ ($\mu<\zeta<0$) satisfies Re $\Sigma_{ee}(\zeta)=0$. In this case, a large-energy-scale kink can be created at $\omega=\zeta$ since the band energy is elevated for $\omega\geq\zeta$ but lowered for $\omega\leq\zeta$. Note that the large-energy-scale kink was previously suggested for the high-T_C cuprates, according to detailed analysis of the ARPES intensity map.[11,12]

In order to roughly simulate the self-energy in the case of Fe(110), we employed a phenomenological analytic function[64–67]

$$\Sigma'(\omega)=\frac{-\beta\zeta^3\omega}{2(\omega-i\zeta)^2}. \quad (3)$$

Here, the parameter $\pm\zeta$ provides a characteristic energy that satisfies Re $\Sigma'(\pm\zeta)=0$. If $\mu<\zeta<0$ is satisfied, the large-energy-scale kink structure can be created due to the self-energy correction.

Based on the model self-energy, the coupling parameter can be calculated as $\lambda'=-(\partial\,\mathrm{Re}\,\Sigma'/\partial\omega)_{\omega=0}=-\beta\zeta/2$. Using the experimentally obtained $\beta\sim 3.6$ eV^{-1} and $\lambda_{ee}\sim 1.7$ (for λ'), we may estimate $\zeta=-0.94$ eV, which is indeed higher than the band bottom energy of −1.8 eV. Figure 7(a) shows simulated $A(k,\omega)$ and Figure 7(b) shows Re Σ' and Im Σ'. We used $f(k)$ in Fig. 2 as a noninteracting band [dashed parabolic band in Fig. 7(a)]. Broadening due to the energy resolution $\Delta E=15$ meV was taken into account as a constant background for Im Σ'.

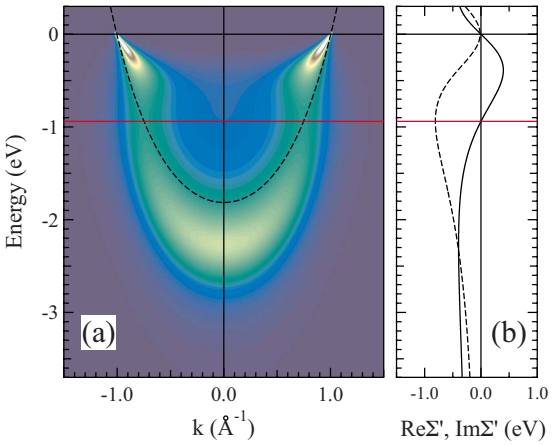

FIG. 7. (Color online) (a) Simulated $A(k,\omega)$ based on a model self-energy Σ'. The dashed line indicates the assumed noninteracting band, which was $f(k)$ as determined in Fig. 2. (b) Real (solid line) and imaginary (dashed line) parts of the self-energy Σ'. Energy-constant lines in red indicate $\zeta=-0.94$ eV.

Near E_F, there was a sharp quasiparticle band whose intensity decreased rapidly with decreasing energy. A broad kink was recognized at an energy of $\zeta=-0.94$ eV, where Re Σ' crossed zero and $|\mathrm{Im}\,\Sigma'|$ reached its maximum. However, this kink was not accessible in the present ARPES measurements due to significant linewidth broadening, reduction in the peak intensity, and interference from other dispersive energy bands [Fig. 3(a)]. Our model simulation indicated that the Fermi velocity was reduced by $\sim 1/3$ while the band energy at the bottom of the band dispersion was lowered by $\sim 30\%$.

A rigorous theoretical calculation incorporating with the one-step photoemission process is highly desirable in order to further understand energy shifts and linewidth broadening of the ARPES spectra. Although iron is considered to be a well-known and well-studied magnet, electron correlation in the Fe 3*d* band continues to provide a fundamental theoretical challenge.

V. CONCLUSION

We performed high-resolution ARPES measurements on an Fe(110) bulk single crystal at low temperature, and examined the spectral shape of a bulk-derived majority-spin band on an FS surrounding the Γ point. The observed group velocity was reduced by a factor of $1/(1+\lambda_{ee})=1/2.7=0.37$ compared with that given by an LSDA calculation. The coupling parameter due to the electron-electron interaction was estimated to be $\lambda_{ee}=1.7\pm 0.1$. A weak kink structure was observed in the energy-band dispersion at ~-40 meV and

was attributed to the electron-phonon interaction. The coupling parameter for the electron-phonon interaction $\lambda_{ep}=0.16\pm0.02$ was much smaller than λ_{ee}. The effective mass enhancement ($m^*/m_b=2.9$) for this band was mainly derived from the renormalization due to the electron-electron interaction. Using EDC analysis, we could not identify a kink structure due to the electron-magnon interaction at energies above ~-300 meV.

In this study, we clarified several important points of line-shape analysis based on EDC and MDC. Further high-resolution ARPES studies of many-body interactions in Fe are needed to clarify the k, spin, and Fermi-surface sheet dependences of the coupling parameters.

ACKNOWLEDGMENTS

We thank the N-BARD of Hiroshima University for supplying liquid helium. The synchrotron radiation experiments were carried out with the approval of HSRC (Proposal No. 04-A-58). We also thank J. Schäfer and R. Clässen for helpful discussions of line-shape analysis and surface resonance states in Fe. We are grateful to Hirashima and Naito for discussions regarding the theoretical calculation of the spin wave. We thank S. Negishi, M. Higashiguchi, and Y. Miura for technical support.

APPENDIX A

Here we describe a self-energy condition for a symmetric MDC, and a relation between spectral linewidth and $2|\mathrm{Im}\,\Sigma|$. Near the Fermi level, we may expand the noninteracting band as $\varepsilon_k^0\sim\hbar v_F^0(|k|-k_F)$. The spectral function for $0<k$ is written as

$$A(k,\omega)=-\frac{1}{\pi}\frac{\mathrm{Im}\,\Sigma(k,\omega)}{[\omega-\varepsilon_k^0-\mathrm{Re}\,\Sigma(k,\omega)]^2+[\mathrm{Im}\,\Sigma(k,\omega)]^2}$$
$$=\frac{1}{\pi\hbar v_F^0}\frac{\eta}{(k-k_\omega)^2+\eta^2}\equiv I_\omega(k), \qquad \text{(A1)}$$

where $k_\omega\equiv k_F-[\omega-\mathrm{Re}\,\Sigma(k,\omega)]/\hbar v_F^0$ and $\eta\equiv|\mathrm{Im}\,\Sigma(k,\omega)|/\hbar v_F^0$. Fixing the energy at $\omega=\varepsilon^*$ and assuming that k is a variable, $I_{\varepsilon^*}(k)$ gives a MDC. If we can neglect the k dependence of the self-energy, namely, assume a local interaction, we have $\Sigma(k,\omega)\sim\Sigma(\omega)$. Then, the MDC is reduced to a Lorentzian with a peak position at $k=k_{\varepsilon^*}\sim k_F-[\varepsilon^*-\mathrm{Re}\,\Sigma(\varepsilon^*)]/\hbar v_F^0$ and a width of $\delta k\sim 2\eta=2|\mathrm{Im}\,\Sigma(\varepsilon^*)|/\hbar v_F^0$.

In the ARPES experiments, we observed renormalized energy-band dispersion. The renormalized energy-band position ε_k^* is given by solving the equation $\varepsilon_k^*-\varepsilon_k^0-\mathrm{Re}\,\Sigma(\varepsilon_k^*)=0$. By taking a partial derivative with respect to k, we obtain $(\frac{\partial\varepsilon_k^*}{\partial k})[1-\frac{\partial\,\mathrm{Re}\,\Sigma(\varepsilon_k^*)}{\partial\varepsilon_k^*}]=(\frac{\partial\varepsilon_k^0}{\partial k})$. The gradient of the renormalized band near E_F is, therefore, given by $(\frac{\partial\varepsilon_k^*}{\partial k})\sim\frac{\hbar v_F^0}{1+\lambda}$, where $\lambda=-\frac{\partial\,\mathrm{Re}\,\Sigma(\varepsilon_k^*)}{\partial\varepsilon_k^*}$ and $\hbar v_F^0=(\frac{\partial\varepsilon_k^0}{\partial k})$.

In this study, the linewidth was evaluated using the formula $\Gamma=(\frac{\partial\varepsilon}{\partial k})\cdot\delta k$. If we use a renormalized energy-band dispersion ε_k^*, we have $\Gamma^*(\varepsilon)=(\frac{\partial\varepsilon_k^*}{\partial k})\cdot\delta k\sim\frac{\hbar v_F^0}{1+\lambda}\cdot\frac{2|\mathrm{Im}\,\Sigma(\varepsilon)|}{\hbar v_F^0}=\frac{2|\mathrm{Im}\,\Sigma(\varepsilon)|}{1+\lambda}$. Note that the imaginary part of the self-energy $2|\mathrm{Im}\,\Sigma(\varepsilon)|$ is not equal to $\Gamma^*(\varepsilon)$ in this case. On the other hand, if we use the group velocity of the noninteracting band ε_k^0, we have $\Gamma(\varepsilon)=(\frac{\partial\varepsilon_k^0}{\partial k})\cdot\delta k\sim\hbar v_F^0\cdot\frac{2|\mathrm{Im}\,\Sigma(\varepsilon)|}{\hbar v_F^0}=2|\mathrm{Im}\,\Sigma(\varepsilon)|$.

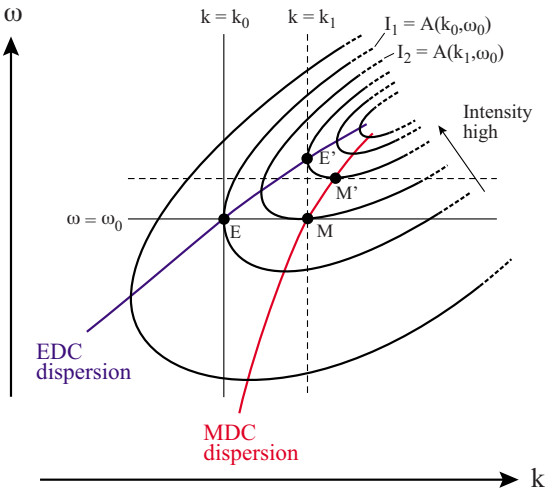

FIG. 8. (Color online) Schematic contour plot of $A(k,\omega)$ corresponding to the ARPES results. The EDC and MDC analyses give different energy-band dispersions for geometric reasons.

APPENDIX B

This section describes why the energy-band dispersions obtained from MDC and EDC analyses were different, using a schematic contour plot of the spectral intensity $I=A(k,\omega)$ in Fig. 8. In EDC analysis, we fix $k=k_0$, and search for the maximum value of I. The energy of the EDC peak position $\omega=\omega_0$ satisfies $\frac{\partial I}{\partial\omega}=\frac{\partial A}{\partial\omega}|_{(k,\omega)=(k_0,\omega_0)}=0$. The peak positions determined by EDC analysis are the points of contact between the $k=k_0$ line and a contour defined by $I_1=A(k_0,\omega_0)=A(k,\omega)$(=constant) (point E in Fig. 8). On the other hand, the peak positions determined by MDC analysis are the points of contact between $\omega=\omega_0$ and a contour defined by $I_2=A(k_1,\omega_0)=A(k,\omega)$(=constant) (point M in Fig. 8). Along the $\omega=\omega_0$ line, $k=k_1$ satisfies $\frac{\partial I}{\partial k}=\frac{\partial A}{\partial k}|_{(k,\omega)=(k_1,\omega_0)}=0$. In general, points E and M are different. The band dispersion given by EDC analysis (E-E′ in Fig. 8) is therefore different from that given by MDC analysis (M-M′ in Fig. 8). As the linewidth broadening becomes significant away from E_F, there is a larger spacing between the contours, and the distance between the band points given by EDC and MDC analysis become larger in the (k,ω) plane. The energy-band dispersions given by EDC and MDC analysis may be close, if the spectral feature is sharp enough or the spacing of the contour plots is small enough, however these conditions depend on the detailed energy and k dependences of the spectral function $A(k,\omega)$.

APPENDIX C

We consider the temperature dependence of the kink structure based on the formula given by Grimvall (Ref. 56). The temperature dependence of the coupling parameter (or

the magnitude of the kink structure) is given by

$$\lambda(T) = -\left.\frac{\partial\, \mathrm{Re}\, \Sigma_{ep}(\omega, \mathrm{T})}{\partial \omega}\right|_{\omega=0} = 2\int_0^{\hbar\omega_{\max}} \frac{\alpha^2 F(\nu)}{\nu} G\left(\frac{\nu}{k_B T}\right) d\nu, \tag{C1}$$

where

$$G(1/t) = 4\left(\frac{1}{\pi t}\right)^2 \sum_{n=0}^{\infty} \frac{2n+1}{\left[(2n+1)^2 + \left(\frac{1}{\pi t}\right)^2\right]^2} \tag{C2}$$

and $t \equiv \frac{k_B T}{\nu}$. Figure 9 shows λ calculated as a function of T (Ref. 68). Here, we used $\alpha^2 F(\nu)$ (inset of Fig. 9) that was used in the calculation of $2|\mathrm{Im}\, \Sigma_{ep}(\omega)|$. On heating, the λ value initially increases slightly, reaching a maximum at ~62 K and then decreases. Note that λ=0.20 at 90 K is nearly equal to λ=0.19 at 0 K. Therefore, it is reasonable to assume that the experimentally evaluated λ at ~90 K is almost the same as it is at 0 K. The calculated λ_{ep} is slightly larger than the experimental one, implying that the assumed Eliashberg function is not fully optimized. Note that we assumed α^2 is a constant in this study.

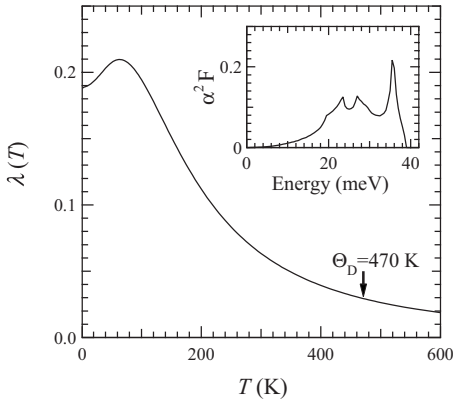

FIG. 9. Calculated λ as a function of temperature. Θ_D indicates the Debye temperature of Fe. The inset shows the Eliashberg function ($\alpha^2 F$) assumed in the present calculations.

*Present address: Fachbereich Physik, Universität Duisburg-Essen, Germany.
†Corresponding author; kshimada@hiroshima-u.ac.jp
‡Present address: Institute of Scientific and Industrial Research, Osaka University, Japan.

[1] P. Nozières and D. Pines, *The Theory of Quantum Liquids* (Perseus Books, Cambridge, Massachusetts, 1966).
[2] *Very High Resolution Photoelectron Spectroscopy*, Lecture Notes Physics Vol. 715, edited by S. Hüfner (Springer-Verlag, Berlin, 2007).
[3] T. Valla, A. V. Fedorov, P. D. Johnson, and S. L. Hulbert, Phys. Rev. Lett. **83**, 2085 (1999).
[4] J. Shi, S.-J. Tang, B. Wu, P. T. Sprunger, W. L. Yang, V. Brouet, X. J. Zhou, Z. Hussain, Z.-X. Shen, Z. Zhang, and E. W. Plummer, Phys. Rev. Lett. **92**, 186401 (2004).
[5] G. Nicolay, F. Reinert, S. Schmidt, D. Ehm, P. Steiner, and S. Hüfner, Phys. Rev. B **62**, 1631 (2000).
[6] A. Eiguren, B. Hellsing, F. Reinert, G. Nicolay, E. V. Chulkov, V. M. Silkin, S. Hüfner, and P. M. Echenique, Phys. Rev. Lett. **88**, 066805 (2002).
[7] M. Higashiguchi, K. Shimada, K. Nishiura, X. Y. Cui, H. Namatame, and M. Taniguchi, Phys. Rev. B **72**, 214438 (2005).
[8] M. R. Norman, H. Ding, H. Fretwell, M. Randeria, and J. C. Campuzano, Phys. Rev. B **60**, 7585 (1999).
[9] A. A. Kordyuk, S. V. Borisenko, A. Koitzsch, J. Fink, M. Knupfer, and H. Berger, Phys. Rev. B **71**, 214513 (2005).
[10] C. Kim, S. R. Park, C. S. Leem, D. J. Song, H. U. Jin, H.-D. Kim, F. Ronning, and C. Kim, Phys. Rev. B **76**, 104505 (2007).
[11] B. P. Xie, K. Yang, D. W. Shen, J. F. Zhao, H. W. Ou, J. Wei, S. Y. Gu, M. Arita, S. Qiao, H. Namatame, M. Taniguchi, N. Kaneko, H. Eisaki, K. D. Tsuei, C. M. Cheng, I. Vobornik, J. Fujii, G. Rossi, Z. Q. Yang, and D. L. Feng, Phys. Rev. Lett. **98**, 147001 (2007).
[12] W. Meevasana, F. Baumberger, K. Tanaka, F. Schmitt, W. R. Dunkel, D. H. Lu, S.-K. Mo, H. Eisaki, and Z.-X. Shen, Phys. Rev. B **77**, 104506 (2008).
[13] J. Callaway and C. S. Wang, Phys. Rev. B **16**, 2095 (1977).
[14] J. Redinger, C. L. Fu, A. J. Freeman, U. König, and P. Weinberger, Phys. Rev. B **38**, 5203 (1988).
[15] D. E. Eastman, F. J. Himpsel, and J. A. Knapp, Phys. Rev. Lett. **44**, 95 (1980).
[16] A. M. Turner and J. L. Erskine, Phys. Rev. B **30**, 6675 (1984).
[17] A. M. Turner, A. W. Donoho, and J. L. Erskine, Phys. Rev. B **29**, 2986 (1984).
[18] E. Kisker, K. Schröder, W. Gudat, and M. Campagna, Phys. Rev. B **31**, 329 (1985).
[19] Y. Sakisaka, T. Rhodin, and D. Mueller, Solid State Commun. **53**, 793 (1985).
[20] H. Kato, T. Ishii, S. Masuda, Y. Harada, T. Miyano, T. Komeda, M. Onchi, and Y. Sakisaka, Phys. Rev. B **32**, 1992 (1985).
[21] Y. Sakisaka, T. Maruyama, H. Kato, Y. Aiura, and H. Yanashima, Phys. Rev. B **41**, 11865 (1990).
[22] A. Santoni and F. J. Himpsel, Phys. Rev. B **43**, 1305 (1991).
[23] J. Schäfer, D. Schrupp, E. Rotenberg, K. Rossnagel, H. Koh, P. Blaha, and R. Claessen, Phys. Rev. Lett. **92**, 097205 (2004).
[24] J. Schäfer, M. Hoinkis, E. Rotenberg, P. Blaha, and R. Claessen, Phys. Rev. B **72**, 155115 (2005).
[25] J. Sánchez-Barriga, J. Fink, V. Boni, I. Di Marco, J. Braun, J. Minár, A. Varykhalov, O. Rader, V. Bellini, F. Manghi, H. Ebert, M. I. Katsnelson, A. I. Lichtenstein, O. Eriksson, W. Eberhardt, and H. A. Dürr, Phys. Rev. Lett. **103**, 267203 (2009).
[26] X. Y. Cui, K. Shimada, Y. Sakisaka, H. Kato, Y. Aiura, M. Higashiguchi, Y. Miura, H. Namatame, and M. Taniguchi, Physica B **383**, 146 (2006).
[27] X. Y. Cui, K. Shimada, Y. Sakisaka, H. Kato, Y. Aiura, M. Higashiguchi, Y. Miura, H. Namatame, and M. Taniguchi, J. Magn. Magn. Mater. **310**, 1617 (2007).

[28] X. Y. Cui, K. Shimada, M. Hoesch, Y. Sakisaka, H. Kato, Y. Aiura, M. Higashiguchi, Y. Miura, H. Namatame, and M. Taniguchi, Surf. Sci. **601**, 4010 (2007).
[29] C. S. Fadley, D. A. Shirley, A. J. Freemen, P. S. Bagus, and J. V. Mallow, Phys. Rev. Lett. **23**, 1397 (1969).
[30] S. Hüfner and G. K. Wertheim, Phys. Lett. A **51**, 299 (1975).
[31] M. Plihal, D. L. Mills, and J. Kirschner, Phys. Rev. Lett. **82**, 2579 (1999).
[32] M. R. Vernoy and H. Hopster, Phys. Rev. B **68**, 132403 (2003).
[33] W. X. Tang, Y. Zhang, I. Tudosa, J. Prokop, M. Etzkorn, and J. Kirschner, Phys. Rev. Lett. **99**, 087202 (2007).
[34] S. V. Halilov, H. Eschrig, A. Y. Perlov, and P. M. Oppeneer, Phys. Rev. B **58**, 293 (1998).
[35] J. W. Lynn, Phys. Rev. **11**, 2624 (1975).
[36] C.-K. Loong, J. M. Carpenter, J. W. Lynn, R. A. Robinson, and H. A. Mook, J. Appl. Phys. **55**, 1895 (1984).
[37] J. A. Blackman, T. Morgan, and J. F. Cooke, Phys. Rev. Lett. **55**, 2814 (1985).
[38] D. McKenzie Paul, P. W. Mitchell, H. A. Mook, and U. Steigenberger, Phys. Rev. **38**, 580 (1988).
[39] M. Naito and D. S. Hirashima, J. Phys. Soc. Jpn. **76**, 044703 (2007).
[40] K. Shimada, M. Arita, Y. Takeda, H. Fujino, K. Kobayashi, T. Narimura, H. Namatame, and M. Taniguchi, Surf. Rev. Lett. **9**, 529 (2002).
[41] Y. Aiura, H. Bando, T. Miyamoto, A. Chiba, R. Kitagawa, S. Maruyama, and Y. Nishihara, Rev. Sci. Instrum. **74**, 3177 (2003).
[42] The temperature measured by the thermocouple connected to the manipulator indicated 10 K. However, we could trace energy-band dispersion up to ~+35 meV above E_F. It clearly shows that the actual sample temperature was much higher than 10 K. Assuming a relation, $5k_BT=35$ meV (Ref. 69), one can estimate the sample temperature as $T\sim 90$ K. The estimate is consistent with the Fermi edge fit giving $T\sim 90$ K. Although the temperature estimate may have 10% error (± 10 K), it does not alter the evaluated energy dependences of $2|\mathrm{Im}\,\Sigma|$ and $\mathrm{Re}\,\Sigma$.
[43] S. Hüfner, *Photoelectron Spectroscopy*, 3rd ed. (Springer-Verlag, Berlin, 2003).
[44] In our previous study (Ref. 28), we assumed the inner potential as $V_0=14.8$ eV, which was determined for a Fe(110) thin film grown on W(110) (Ref. 24). The inner potential is much larger than the value obtained for the bulk sample ($V_0=8.9$ eV) (Ref. 19). The discrepancy of the value may be solved if we consider that the lattice constant of the thin film is expanded perpendicular to the surface by ~2%.
[45] All of the band-structure calculations presented here have been performed within the local-spin-density approximation using the full-potential linearized augmented-plane-wave method implemented with the HiLAPW program package.
[46] S. Sahrakorpi, M. Lindroos, and A. Bansil, Phys. Rev. B **66**, 235107 (2002).
[47] N. V. Smith, P. Thiry, and Y. Petroff, Phys. Rev. B **47**, 15476 (1993).
[48] T.-C. Chiang, Chem. Phys. **251**, 133 (2000).
[49] A. Hofmann, X. Y. Cui, J. Schäfer, S. Meyer, P. Höpfner, C. Blumenstein, M. Paul, L. Patthey, E. Rotenberg, J. Bünemann, F. Gebhard, T. Ohm, W. Weber, and R. Claessen, Phys. Rev. Lett. **102**, 187204 (2009).
[50] X. Y. Cui, E. E. Krasovskii, V. N. Strocov, A. Hofmann, J. Schäfer, R. Claessen, and L. Patthey, Phys. Rev. B **81**, 245118 (2010).
[51] E. E. Krasovskii, K. Rossnagel, A. Fedorov, W. Schattke, and L. Kipp, Phys. Rev. Lett. **98**, 217604 (2007).
[52] V. N. Strocov, J. Electron Spectrosc. Relat. Phenom. **130**, 65 (2003).
[53] S. Doniach and M. Sunjic, J. Phys. C **3**, 285 (1970).
[54] C. Kittel, *Introduction to Solid State Physics*, 6th ed. (Wiley, New York, 1986).
[55] F. J. Himpsel, K. N. Altmann, G. J. Mankey, J. E. Ortega, and D. Y. Petrovykh, J. Magn. Magn. Mater. **200**, 456 (1999).
[56] G. Grimvall, *The Electron-Phonon Interaction in Metals* (North-Holland, Amsterdam, New York, Oxford, 1981).
[57] A. A. Lysykh, I. K. Yanson, O. I. Shklarevskii, and Yu. G. Naidyuk, Sov. J. Low Temp. Phys. **6**, 224 (1980).
[58] G. G. Lonzarich, J. Magn. Magn. Mater. **45**, 43 (1984).
[59] A. Yamasaki and T. Fujiwara, J. Phys. Soc. Jpn. **72**, 607 (2003).
[60] P. Pou, F. Flores, J. Ortega, R. Pérez, and A. L. Yeyati, J. Phys.: Condens. Matter **14**, L421 (2002).
[61] A. Grechnev, I. DiMarco, M. I. Katsnelson, A. I. Lichtenstein, J. Wills, and O. Eriksson, Phys. Rev. B **76**, 035107 (2007).
[62] N. E. Zein and V. P. Antropov, Phys. Rev. Lett. **89**, 126402 (2002).
[63] A. L. Walter, J. D. Riley, and O. Rader, New J. Phys. **12**, 013007 (2010).
[64] T. Saitoh, A. Sekiyama, T. Mizokawa, A. Fujimori, K. Ito, H. Nakamura, and M. Shiga, Solid State Commun. **95**, 307 (1995).
[65] K. Shimada, T. Mizokawa, K. Mamiya, T. Saitoh, A. Fujimori, K. Ono, A. Kakizaki, T. Ishii, M. Shirai, and T. Kamimura, Phys. Rev. B **57**, 8845 (1998).
[66] M. Arita, K. Shimada, Y. Takeda, M. Nakatake, H. Namatame, M. Taniguchi, H. Negishi, T. Oguchi, T. Saitoh, A. Fujimori, and T. Kanomata, Phys. Rev. B **77**, 205117 (2008).
[67] M. Klein, D. Zur, D. Menzel, J. Schoenes, K. Doll, J. Röder, and F. Reinert, Phys. Rev. Lett. **101**, 046406 (2008).
[68] In the textbook by Grimvall (Ref. 56), one can see a similar figure calculated for the Einstein model (Fig. 5.10 in Ref. 56). The abscissa in the textbook, however, should read $y^{-1}(=k_BT/\hbar\omega_E)$.
[69] T. Greber, T. J. Kreutz, and J. Osterwalder, Phys. Rev. Lett. **79**, 4465 (1997).